Life Sciences 237 (2019) 116941

Contents lists available at ScienceDirect

Life Sciences

journal homepage: www.elsevier.com/locate/lifescie

Mitochondrial pyruvate carrier 2 mediates mitochondrial dysfunction and apoptosis in high glucose-treated podocytes

Jun Feng[1], Yiqiong Ma[1], Zhaowei Chen, Jijia Hu, Qian Yang, Guohua Ding*

Division of Nephrology, Renmin Hospital of Wuhan University, Wuhan, China

ARTICLE INFO

Keywords:
Diabetic kidney disease
Podocytes
Mitochondria
Mitochondrial pyruvate carrier 2
Apoptosis

ABSTRACT

Aims: Podocytes play an important role in the development of diabetic kidney disease (DKD). Mitochondria are the source of energy for cell survival, and mitochondrial abnormalities have been shown to contribute to podocyte injury in DKD. In high glucose (HG)-treated podocytes, mitochondrial function and dynamics are abnormal, and intracellular metabolism is often disrupted. However, the molecular mechanism is still unclear. Mitochondrial pyruvate carrier 2 (MPC2) mediates pyruvate transport from the cytoplasm to the mitochondrial matrix, which determines the cellular energy supply and cell survival. Here, we hypothesize that MPC2 damages mitochondria and induces apoptosis in HG-treated podocytes.

Main methods: We used Western blotting, immunofluorescence and immunoprecipitation to detect the expression of MPC2 in HG-treated podocytes. Pyruvate levels were measured to evaluate metabolic station. Mitochondrial membrane potential (MMP) was measured by inverted fluorescence microscopy and flow cytometry. Mitochondrial morphology was assayed by MitoTracker Red staining, and cellular apoptosis was examined by flow cytometry. Furthermore, we treated podocytes with UK5099 and MPC2 siRNA to assess the outcomes of UK5099 treatment and MPC2 knockdown.

Key findings: Intracellular pyruvate accumulated, the mitochondria were damaged and cellular apoptosis increased in podocytes cultured with HG compared to that in control podocytes. MPC2 acetylation was significantly increased in HG-treated podocytes. Furthermore, the mitochondrial morphology changed, the MMP decreased, and cellular apoptosis increased. Inhibition of MPC2 function by UK5099 or MPC2 knockdown by siRNA produced the same abnormal effects observed following treatment with HG.

Significance: MPC2 may mediate mitochondrial dysfunction in HG-treated podocytes, ultimately leading to cell apoptosis.

1. Introduction

With the increasing morbidity and mortality of diabetes worldwide, diabetic kidney disease (DKD) has become the leading cause of end stage renal disease (ESRD). Approximately half of all new cases of ESRD in America are DKD [1,2]. DKD is the most common microvascular disease in diabetic patients, and diabetes in approximately 40% of patients eventually progresses to DKD [3].

Podocytes, one of three major types of intrinsic cells in the glomerulus, participate in the formation of the glomerular filtration barrier. Energy-dependent actin filaments are mainly involved in maintaining the shape and function of foot processes, which are complex and unique cellular structures in podocytes. Podocytes play an important role in the progression of DKD [4].

In recent years, the role of mitochondria in DKD has attracted extensive attention. Mitochondria are thought of as power plants as they are the energy-producing organelles in the cell. An adequate energy supply ensures normal operation of the kidneys, especially glomerular cells and podocytes [5,6]. Abnormalities in the physiological function and dynamics of mitochondria in podocytes are involved in podocyte injury. Mitochondrial oxidative stress and reactive oxygen species (ROS) are increased in HG-treated podocytes [7]. The effects of DKD on mitochondria are swelling with the loss of cristae, the formation of vacuoles and reduced matrix density. The proportion of fragmented mitochondria was increased significantly in diabetic mice [7,8]. Abnormal activity of key enzymes or factors involved in metabolism in DKD patients has been shown to change the oxygen demand, which altered normal energy production in podocytes, decreasing ATP

* Corresponding author. Division of Nephrology, Renmin Hospital of Wuhan University, Wuhan, 430000, Hubei, China.
E-mail address: ghxding@gmail.com (G. Ding).
[1] Co-first authors.

https://doi.org/10.1016/j.lfs.2019.116941
Received 15 July 2019; Received in revised form 5 October 2019; Accepted 6 October 2019
Available online 10 October 2019
0024-3205/

production compared to that in controls [9,10].

Pyruvate, which is generated by the decomposition of glucose in glycolysis, is an important intermediate for maintaining the stability of mitochondrial biological function. Pyruvate concentration is a potential biomarker of diabetes [11], cardiovascular disease [12] and periodontal disease [13]. In the early stage of DKD, lactic acid and pyruvate accumulate in kidneys [14], and changed pyruvate levels may indicate disordered cellular metabolic stations.

Mitochondrial pyruvate carrier (MPC) is located in the inner mitochondrial membrane (IMM), where it mediates the transport of pyruvate from the cytoplasm to mitochondria. MPC comprises two subunits, MPC1 and MPC2, and the abnormal expression of each of them will lead to MPC dysfunction [15]. MPC plays a role in maintaining the balance of glycolysis and oxidative phosphorylation. Metabolic disorders are often accompanied by abnormal MPC function [16]. MPC is involved in the occurrence and development of a wide range of many diseases, such as pancreatic cancer [17], lung adenocarcinoma [18], Parkinson's disease [19], hepatocarcinoma [20], renal cell carcinoma [21] and diabetic cardiomyopathy [22]. Pyruvate metabolism and oxygen consumption were altered by mitochondrial pyruvate transport blockade in MPC2-deficient mice [23,24]. However, the role of MPC2 in HG-treated podocytes is still unknown. Therefore, we hypothesize that MPC2 mediates abnormal glucose metabolism, ultimately leading to mitochondrial dysfunction and cell apoptosis.

2. Materials and methods

2.1. Cell culture

Conditionally immortalized human podocytes were provided by Dr. Moin A. Saleem (Academic Renal Unit, Southmead Hospital, Bristol, UK). Podocytes were cultured in RPMI 1640 medium (HyClone, USA) containing 10% fetal bovine serum (Gibco, Australia), 100 μg/mL streptomycin, 100 U/mL penicillin G (Thermo, USA) and 1x insulin transferrin-selenium (ITS) (Gibco, USA) proliferated in a 33 °C incubator in 5% CO_2. Then, cells were cultured in ITS-free medium in a 37 °C incubator in 5% CO_2 for one week. The differentiated cells were stimulated with a normal concentration of glucose (5 mM), a high concentration of glucose (30 mM) and the MPC inhibitor UK5099 (30 nM) for 24 h. After stimulation, cells were used for subsequent experiments.

2.2. siRNA transfection

Transfection of MPC2 siRNA (Qiagen) was conducted using HiPerFect Transfection Reagent (Qiagen) according to the manufacturer's instructions. A total of 2×10^5 cells were first seeded in each well of a six-well plate. Then, the cells were transfected with a mixture containing 6 μl MPC2 siRNA solution (10 μM) and 12 μl transfection reagent for two days. The cells were then incubated under normal conditions at 37 °C (target sequences: Hs_BRP44_1: AACCATTGGGACC TAGTTTAT, Hs_BRP44_3:TACCACCGGCTCCTCGATAAA, Hs_BRP44_4: CAGTCTCTCTACATGACTTAA, Hs_BRP44_5:AACAATCTAGATGTGGAC AAA).

2.3. Western immunoblotting

Cells were lysed in cell lysis buffer (Beyotime, China) mixed with protease inhibitor cocktail (Sigma, USA) and PMSF (Beyotime, China) at 100:1:1 on ice. The mixture was extracted after cell lysis and centrifuged at 12000 rpm for 10 min at 4 °C. The supernatants were mixed with SDS-PAGE protein loading buffer (Beyotime, China) and boiled at 100 °C for 10 min. Equal amounts of protein samples were separated through SDS-PAGE and then transferred to 0.2 μm PVDF membranes (Sigma, USA). Membranes were blocked with 5% nonfat milk for 1 h and incubated with primary antibody (MPC2 rabbit monoclonal antibody, 1:500, CST; VDAC1 mouse monoclonal antibody, 1:1000, Abcam; α-tubulin rabbit polyclonal antibody, 1:1000, Proteintech, and acetylated-lysine rabbit antibody, 1:1000, CST) overnight at 4 °C. Next, the membranes were incubated with a secondary antibody, HRP-conjugated goat anti-rabbit/goat anti-mouse IgG (H + L) antibody, for 1 h. The proteins were detected with ECL reagent by a Bio-Rad imaging system.

2.4. Immunoprecipitation

Podocytes were cultured in a Petri dish (NEST, China) with a diameter of 10 cm. After the appropriate treatment, the proteins were extracted and incubated with 5 μl MPC2 rabbit monoclonal antibody (CST, USA) and 30 μl protein A + G agarose suspension beads (calbiochem, USA) while rotating overnight at 4 °C. The beads were washed 3 times and boiled in loading buffer at 100 °C for 10 min. To detect the degree of MPC2 acetylation, the proteins were separated by SDS-PAGE, and the blots were incubated with acetylated lysine rabbit antibody (1:500, CST, USA) overnight at 4 °C. Additional steps followed the protocols for Western immunoblotting.

2.5. Immunofluorescence assay

Cells were plated on the coverslips at the appropriate density. The adhered cells were fixed with 4% paraformaldehyde for 20 min on ice and sealed with 10% BSA for 1 h. Cells were then incubated with MPC2 rabbit polyclonal antibody (1:100, Proteintech, China) and Tom20 mouse monoclonal antibody (1:100, Santa, USA) overnight at 4 °C, and then Alexa Fluor 488-labeled donkey anti-rabbit/mouse immunoglobulin G (H + L) (1:100, Antgene, China) for 60 min at room temperature in the dark. An antifluorescence quenching agent containing DAPI was applied to the coverslips. All microscopic images were recorded by using a confocal microscope or an automatic microscope (Olympus, Japan).

2.6. Pyruvate assay

Cells were seeded evenly into culture plates at the appropriate density. The cells were harvested after a series of treatments, and pyruvate was collected by the introductions for a pyruvate assay kit (Sigma, MAK071, USA). Cells were collected and mixed with 100 μl pyruvate assay buffer. The samples were centrifuged at 13,000 × *g* for 10 min to remove insoluble material. 50 μl of a master reaction mix (46 μl pyruvate assay buffer, 2 μl pyruvate probe solution and 2 μl pyruvate enzyme mix)were added to each of the wells. The cells were mixed well using a horizontal shaker and incubated for 30 min at room temperature. For colorimetric assays, the absorbance at 570 nm was measured using a microplate reader. The pyruvate concentrations of the samples were calculated based on the absorbance of the standards.

2.7. MMP assay

MMP was measured with the unique fluorescence probe JC-1 with an MMP assay kit (Beyotime, China). Cells were stained with JC-1 at 37 °C for 20 min. After incubation, the cells were washed twice. The fluorescent intensity of the cells was observed by inverted fluorescence microscopy (Olympus, Japan). The cells were also resuspended in PBS before analysis with a flow cytometer (BD FACS Calibur, USA). For each cell, the average intensity of green and red fluorescence was determined, and the ratio was calculated.

2.8. MitoTracker red staining

Cells were grown until they had differentiated fully and were then treated as described above. After treatment for 24 h, cells were incubated with 50 nM MitoTracker Red (Yeasen, China) for 20 min in

37 °C incubator, fixed with 4% paraformaldehyde for 20 min on ice, and sealed with antifluorescence quenching agent containing DAPI. The mitochondrial morphology of the podocytes was observed by confocal microscopy (Olympus, Japan). Mitochondrial shape and size including length, aspect ratio (major axes/minor axes), surface area, perimeter and form factor (4π area/perimeter^2), were determined by using Image-Pro software. Five representative images were selected from each group. At least 100 mitochondria were counted in each different group.

2.9. Apoptosis assay

The degree of podocyte apoptosis in vitro was assessed in vitro by flow cytometry (BD FACS Calibur, USA) according to the manufacturer's instructions (Annexin V-ADD Apoptosis Detection Kit I, BD, USA). Each well of a six-well plate was used to hold a sample. After resuspending cells in 100 μl 1x binding buffer, 5 μl AnnexinV-AAD and 5 μl PE was added to each sample, which was incubated for 15 min at room temperature in the dark. Cells were resuspended in 400 μl 1x binding buffer again before the apoptosis assay.

2.10. Statistical analysis

All data represent at least three independent experiments and statistical analyses were performed using GraphPad Prism 6. The statistical significance of differences was determined by Student's two-tailed *t*-test or one-way analysis of variance ($p < 0.05$ indicated statistical significance).

3. Results

3.1. High glucose (HG) induced pyruvate accumulation, MMP reduction and podocyte apoptosis

Podocytes were cultured with a normal level of glucose (NG group), a high level of mannitol (30 mM) (MA group) and a high level of glucose (30 mM) (HG group) for 24 h. The intracellular pyruvate was higher in HG group than in the other groups (Fig. 1A). A decrease in MMP is a hallmark event of early apoptosis. Podocytes were stained with JC-1, a fluorescent probe that aggregates in the mitochondrial matrix and emits red fluorescence when the MMP is high and green fluorescence when the MMP declines. Compared with the green fluorescence intensity in the NG group, that in the HG group was stronger when observed under an inverted fluorescence microscope. In contrast, the red fluorescent intensity was weaker (Fig. 1B). The MMP was also detected by flow cytometry, by which the ratio of red and green fluorescence was determined. Flow cytometry also indicated that the MMP was lower in HG-treated podocytes (Fig. 1C). Podocyte apoptosis was also increased under the high glucose state (Fig. 1D). Taken together, these findings suggest that mitochondrial function was damaged in HG-treated podocytes, which disrupts pyruvate metabolism and cell apoptosis.

3.2. MPC2 acetylation was increased in HG-treated podocytes

Pyruvate, an intermediate in whole cell metabolism, participates in regulating the homeostasis of the intracellular environment. We revealed increased levels of pyruvate in HG-treated podocytes. MPC2 mediates the transport of pyruvate from the cytoplasm to mitochondria. Recent studies found that abnormal MPC2 causes mitochondrial dysfunction. To determine whether MPC2 was related to pyruvate accumulation in HG-treated podocytes, the expression of MPC2 was evaluated. We found that the MPC2 expression did not change with increased concentration of glucose (Fig. 2A). MPC2 expression was also not dependent on the time frame of HG treatment (Fig. 2B). MPC1 expression did not change significantly too (Supplementary data A and B). Immunofluorescent images showed that MPC2 is located in the mitochondria co-stained with a mitochondrial marker Tom20. The MPC2 fluorescent intensity did not change obviously when observed via an immunofluorescence assay (Fig. 2C). Acetylation is a common protein modification, and protein acetylation regulates cellular signaling pathways to produce diverse outcomes. The acetylation of multiple transcription factors was reported to be increased in mice and patients with DKD compared with that in control mice and healthy individuals [25]. Therefore, we explored the acetylation of cellular proteins. Western blotting showed that the levels of cellular protein acetylation increased in HG-treated podocytes and were dependent on the concentration of glucose (Fig. 2D) and the treatment time (Fig. 2E). Then, we hypothesized that MPC2 acetylation would increase in HG-treated podocytes. Our findings confirmed this, and the levels of MPC2 acetylation increased significantly in HG-treated podocytes (Fig. 2F). The above results showed that MPC2 acetylation might affect the normal transport of pyruvate, leading to mitochondrial dysfunction.

3.3. Inhibition of MPC2 function or expression caused mitochondrial dysfunction and cell apoptosis in podocytes

To identify the role of MPC2 in pyruvate transport, we treated podocytes in normal glucose with UK5099 (UK), a specific functional inhibitor of MPC, and MPC2 siRNA (SI) to reduce its expression. MPC2 expression did not change in the UK treated cells, but decreased significantly in the siRNA treated cells (Fig. 3A). DMSO and a transfected scramble control couldn't alter MPC2 expression (Supplementary data C and F). There was no significant change in acetylation level both in DMSO and scramble control groups (Supplementary data D and G). Fluorescent images showed that the MPC2 fluorescent intensity was consistent with the results Western blotting (Fig. 3B). Next, we determined the intracellular pyruvate levels in podocytes after the inhibition of MPC2. Pyruvate levels were increased both in the UK and SI treated cells (Fig. 3C). Then, the MMP was detected and found to be lower in podocytes treated with UK and SI compared to that in untreated podocytes (Fig. 3D and E). Fig. 3F showed that cell apoptosis was increased in the UK and SI treated cells (Fig. 3F). The effect of DMSO and scramble siRNA to cell apoptosis was not obvious (Supplementary data E and H). Altogether, these results showed that the inhibition of MPC2 in podocytes led to pyruvate accumulation, mitochondrial dysfunction and cell apoptosis.

3.4. Change of MPC2 function and expression led to abnormal mitochondrial dynamics in podocytes

Mitochondrial morphology is in dynamic equilibrium within cells and mitochondrial fission and fusion change as the cellular environment changes. Excessive mitochondrial fission is characteristic of mitochondrial dysfunction in diabetic kidneys, especially in podocytes [26,27]. ATP production and oxygen consumption were decreased in HG-treated podocytes [8,10]. Mitochondrial morphology and energy metabolism may be correlated. We next examined the effect of MPC2 on mitochondrial dynamics in podocytes. Mitochondria in different groups were stained by MitoTracker Red and observed by confocal microscopy (Fig. 4A). We then quantified changes in mitochondrial morphology by detecting the length (Fig. 4B), aspect ratio (Fig. 4C), surface area (Fig. 4D), perimeter (Fig. 4E) and form factor (Fig. 4F) of the mitochondria in cultured podocytes. Compared with those in control podocytes, all the mitochondrial morphology-related indicators were decreased in podocytes treated with HG, UK and SI. Therefore, this might indicate that MPC2 inhibition led to mitochondrial fragmentation in podocytes.

4. Discussion

Mitochondrial dysfunction, including metabolic disorder and morphological abnormity, is closely related to cell survival in DKD.

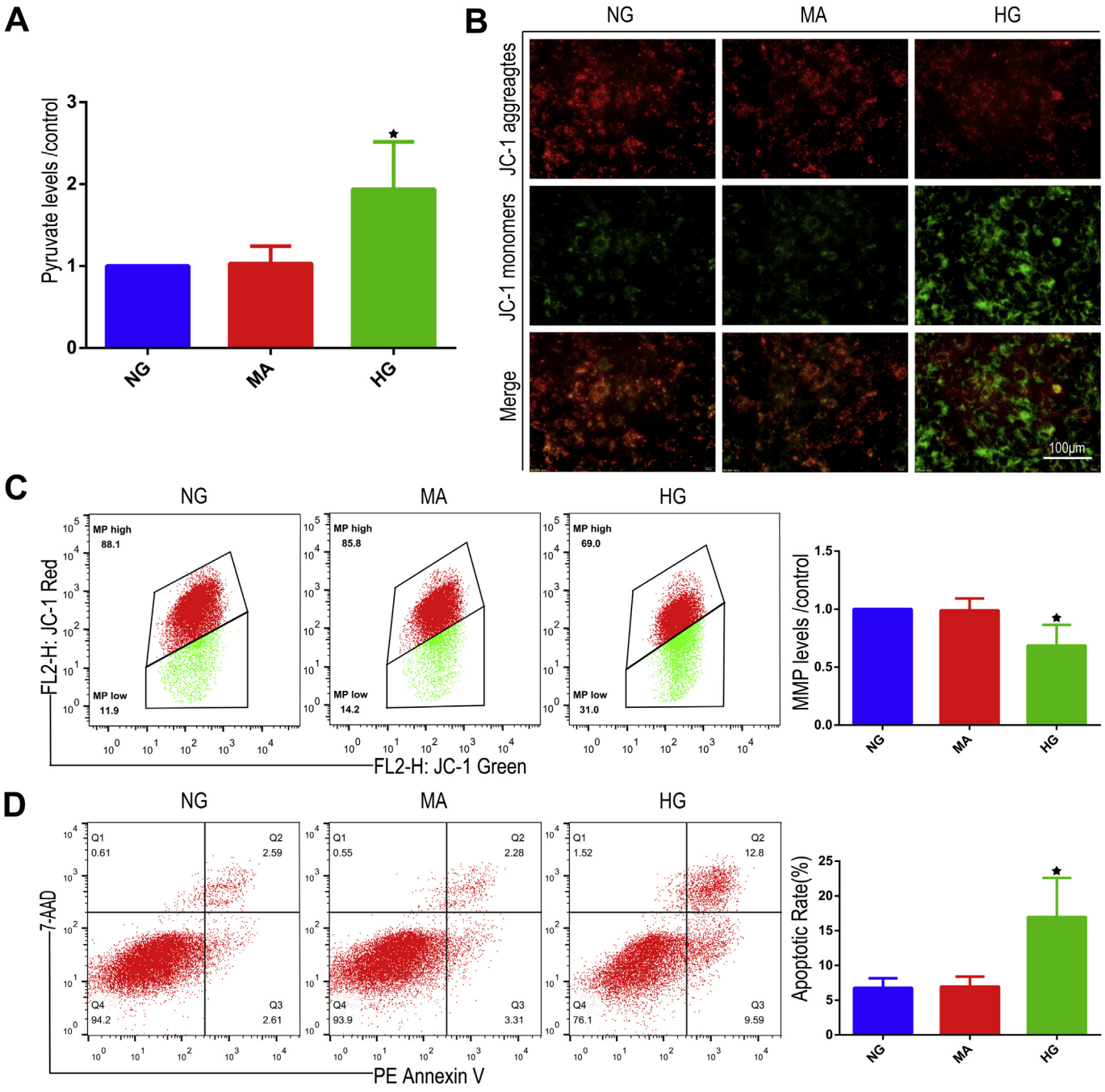

Fig. 1. High glucose induced pyruvate accumulation, MMP reduction and cell apoptosis in podocytes. Podocytes were treated with high levels of mannitol (30 mM) and glucose (30 mM) for 24 h. Podocytes treated with normal levels of glucose were regarded as the control group (NG: control group; MA: high mannitol group; HG: high glucose group). (A) The levels of intracellular pyruvate were detected by using a pyruvate assay kit and a microplate reader. The figure shows the semi-quantitative analysis of pyruvate concentrations in different groups. n = 3, ★$p < 0.05$ compared with NG group. (B) The MMP was determined by JC-1 staining. Red and green fluorescence was observed by an inverted fluorescence microscope (original magnification, 400×). (C) MMP levels were also detected by flow cytometry. n = 3, ★$p < 0.05$ compared with the NG group. (D)The podocyte apoptotic rate was evaluated by flow cytometry. n = 3, ★$p < 0.05$ compared with the NG group. (For interpretation of the references to color in this figure legend, the reader is referred to the Web version of this article.)

However, the mechanisms of mitochondria-related cellular damage are still not well understood, especially that in podocytes. Our study identified a correlation between MPC2 with mitochondrial dysfunction and cell apoptosis in HG-treated podocytes. We firstly found that MPC2 acetylation was increased in podocytes cultured with HG. When MPC2 was supressed by UK5099 and siRNA, podocytes exhibited similar effects that included pyruvate accumulation, decreased MMP and increased cell death, like podocytes cultured in HG. This suggests that acetylated MPC2 does not transport pyruvate. As a result, pyruvate produced by the glycolysis process accumulated in the cytoplasm, which was accompanied by mitochondrial malfunction, such as decreased ATP production, a decrease in MMP and mitochondrial fragmentation.

MPC acts as a gatekeeper for the entrance of pyruvate into the mitochondria and has a certain regulatory effect on energy supply [28,29]. Due to the special structure and physiological role of MPC, it is studied in various fields and has been shown to exert different effects in various disease models. This may be related to the specific metabolic

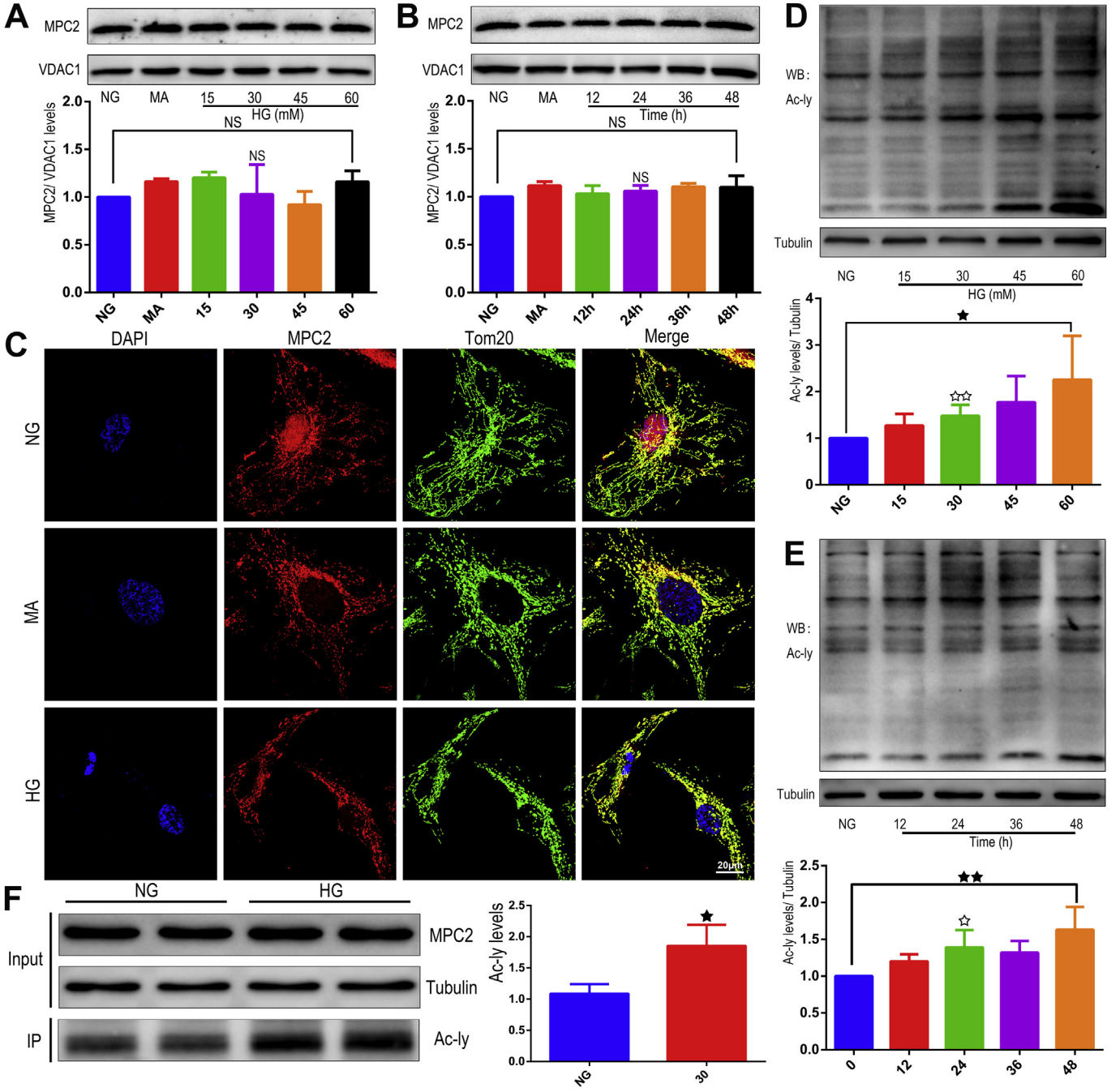

Fig. 2. MPC2 acetylation were increased in high glucose-treated podocytes. Podocytes were treated with different concentrations of glucose for different lengths of time. (A) Representative Western blots showing MPC2 expression in cultured podocytes stimulated with a series of concentrations of glucose for 24 h and semi-quantification of these results. n = 3, $p > 0.05$ compared with the NG group. There was no significant difference in MPC expression between groups. (B) Representative Western blots showing MPC2 expression in cultured podocytes stimulated with a high level of glucose (30 mM) for various lengths of time and the semiquantification of these results. n = 3, $p > 0.05$ compared with the NG group. (C) Immunofluorescence of MPC2 in cultured podocytes in 3 groups (original magnification, 1000×). (D) Representative Western blots showing whole cell acetylation levels in HG-induced podocytes treated with different concentrations of glucose for 24 h and semiquantification of these results. n = 4, ★$p < 0.05$ compared with all groups by ANOVA of the means of multiple-samples. ☆☆$p < 0.01$ compared with the NG group. (E) Representative Western blots showing whole cell acetylation levels in podocytes treated with a high levels of glucose (30 mM) for different lengths of time and semiquantification of these results. n = 4, ★★$p < 0.01$ compared with all groups by ANOVA of the means of multiple samples. ☆$p < 0.05$ compared with group treated for 24 h. (F) Representative Western blots showing MPC2 acetylation detected by IP and semiquantification of these results. Podocytes were treated with a high level of glucose (30 nM) for 24 h n = 3, ★$p < 0.05$ compared with the NG group.

pattern of ATP production in cells, for example, oxidative phosphorylation, fatty acid metabolism and aerobic glycolysis. MPC consists of two subunits, MPC1 and MPC2. Previous studies reported different roles for each subunit, but a consensus on this issue has not yet been determined reached. Schell et al. found that the expression of MPC1 was absent or downregulated in multiple cancers, especially in colon carcinoma cell lines and that the loss of MPC activity was correlated with mitochondrial pyruvate oxidation and poor prognosis [30]. Loss of MPC activity in mice with liver-specific MPC2 deficiency could impair pyruvate-driven gluconeogenesis by decreasing pyruvate uptake and affecting blood glucose [23]. Interestingly, MPC activity was decreased without the change of MPC1 and MPC2 expression in diabetic hearts

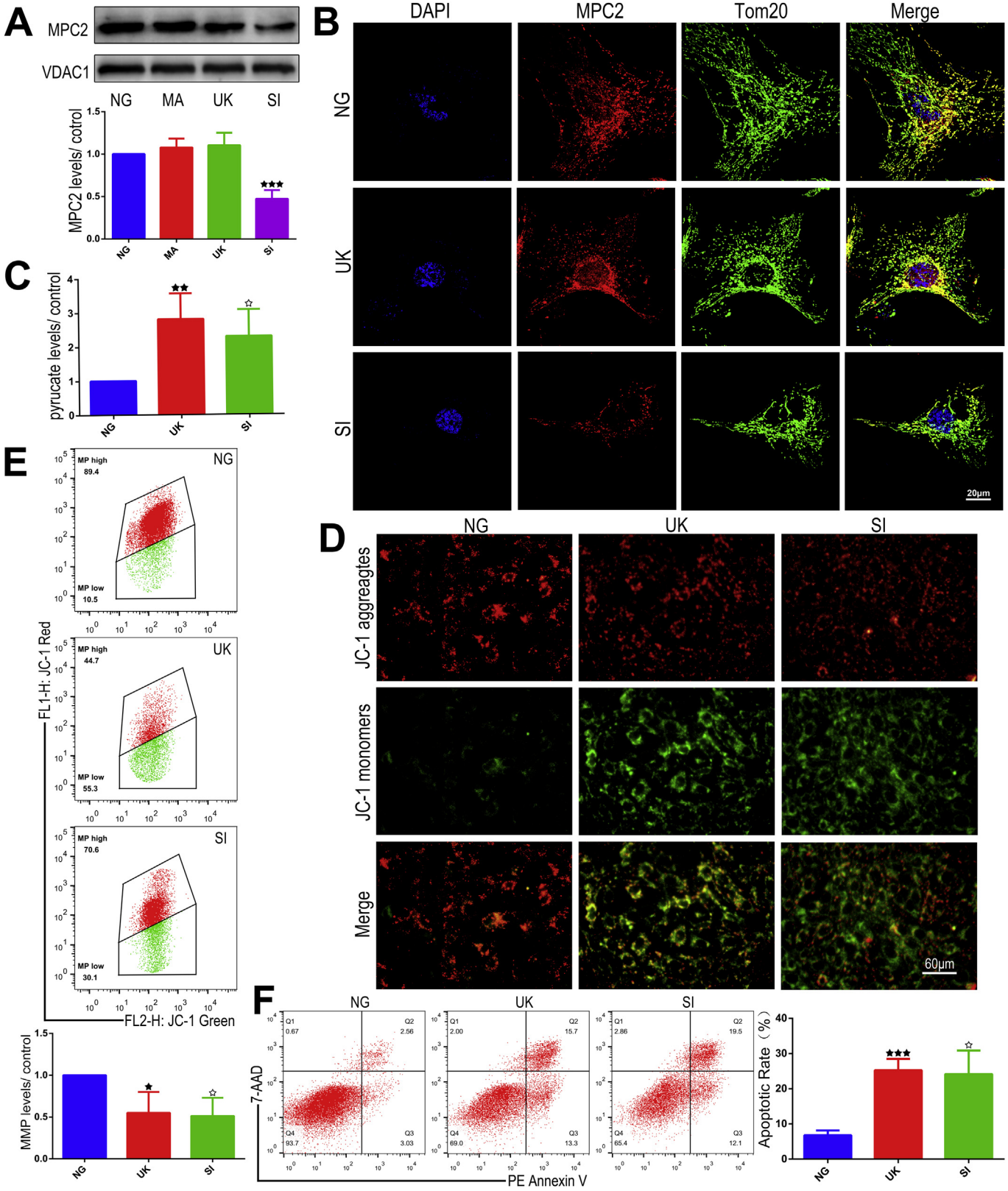

Fig. 3. Inhibition of MPC2 function or expression caused mitochondrial dysfunction and cell apoptosis in podocytes. Podocytes were treated with the MPC inhibitor, UK5099(30 nM) or transfected with MPC2 siRNA. NG: control group; MA: high mannitol group; UK: UK5099 group; SI: MPC2 siRNA group. (A) Representative Western blots showing MPC2 expression in podocytes treated with UK5099 or MPC2 siRNA and semiquantification of these results. n = 3, ★★★$p < 0.001$ compared with the NG group. (B) Immunofluorescence results of MPC2 in podocytes in the NG, UK and SI group (original magnification, 1000×). (C) The levels of intracellular pyruvate in cultured podocytes after simulation. n = 3, ★★$p < 0.01$ compared with NG group; ☆$p < 0.05$ compared with NG group. (D) Representative images showing JC-1 staining in different groups of podocytes to determine the MMP screened by an inverted fluorescence microscope (original magnification, 400×). (E) Images showing JC-1 staining in different groups detected by flow cytometry to determine the MMP. n = 3, ★$p < 0.05$ compared with NG group; ☆$p < 0.05$ compared with NG group. (F) Flow cytometry analysis of apoptosis in cultured podocytes in different groups and quantitation of these results. n = 3, ★★★$p < 0.001$ compared with NG group; ☆$p < 0.05$ compared with NG group.

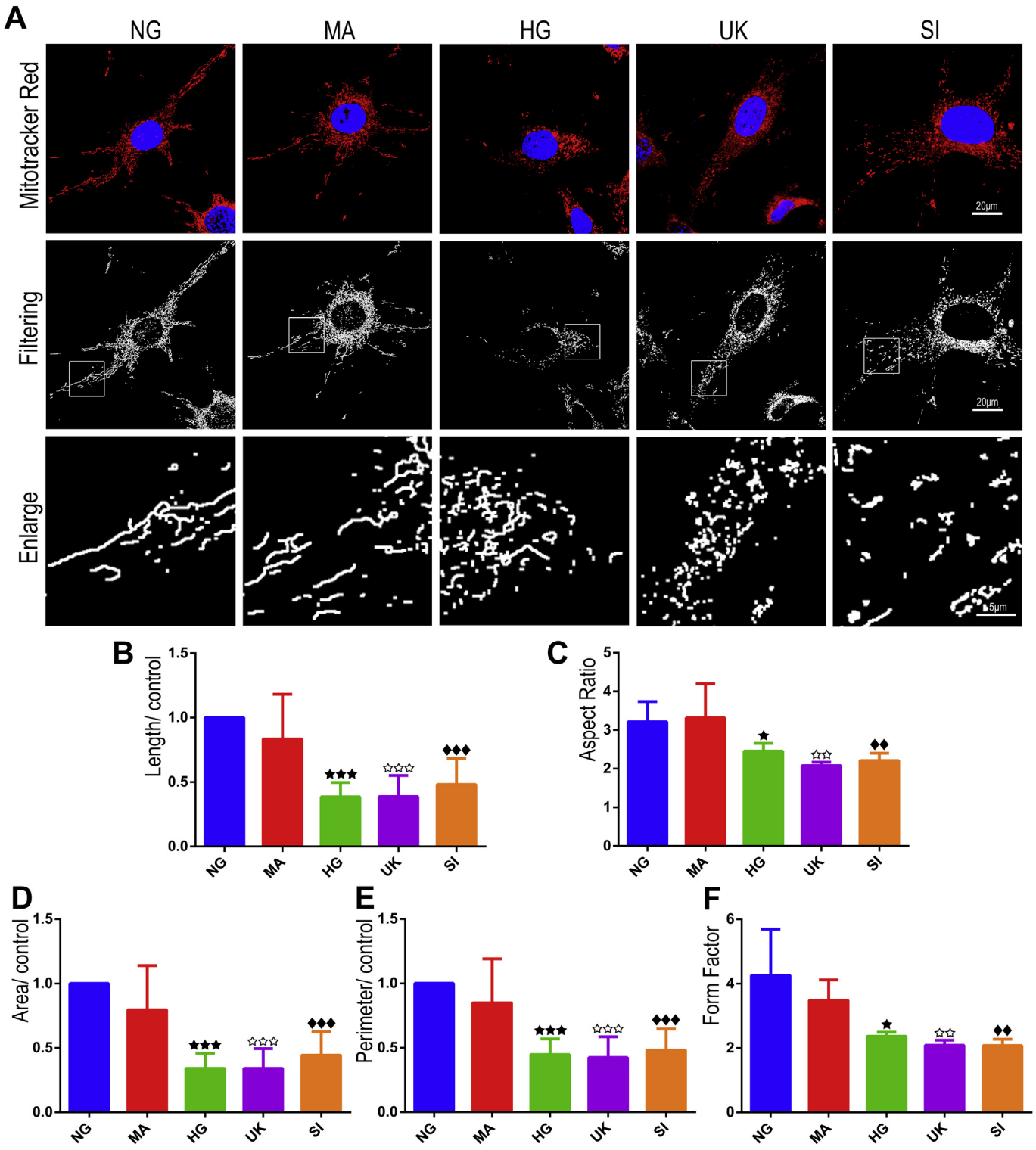

Fig. 4. Change of MPC2 expression and function led to abnormal mitochondrial dynamics in podocytes. Podocytes were treated with a normal level of glucose (NG group), a high level of mannitol (MA group), a high level of glucose (HG group), UK5099 (UK group) and siRNA (SI group). Podocytes were stained with MitoTracker Red (red) and DAPI (blue). (A) Representative immunofluorescence micrographs of cells in different groups (original magnification, 1000×). Images were filtered by Image Pro. (B) Data showing mitochondrial length in each group measured by Image Pro analysis. n = 5, ★★★$p < 0.001$ compared with NG group; ☆☆☆$p < 0.001$ compared with NG group; ◆◆◆$p < 0.001$ compared with NG group. (C) Aspect ratios were quantified for podocytes treated with each condition. n = 5, ★$p < 0.05$ compared with NG group; ☆☆$p < 0.01$ compared with NG group; ◆◆$p < 0.01$ compared with NG group. (D) The mitochondrial surface area was quantified and related to that of the control group for podocytes treated with each condition. n = 5, ★★★$p < 0.001$ compared with NG group; ☆☆☆$p < 0.001$ compared with NG group; ◆◆◆$p < 0.001$ compared with NG group. (E) The perimeter of mitochondria in podocytes treated with each condition was quantified. n = 5, ★★★$p < 0.001$ compared with NG group; ☆☆☆$p < 0.001$ compared with NG group; ◆◆◆$p < 0.001$ compared with NG group. (F) The form factor of mitochondria in different groups was quantified and related to that of the control group. n = 5, ★$p < 0.05$ compared with NG group; ☆☆$p < 0.01$ compared with NG group; ◆◆$p < 0.01$ compared with NG group. (For interpretation of the references to color in this figure legend, the reader is referred to the Web version of this article.)

[22]. In our study, we focused on the role of MPC2 and found no significant change in the MPC2 expression in podocytes treated with HG or UK5099 compared to that in control cells, but observed pyruvate accumulation. The activity of MPC in podocytes might be influenced by protein-protein interactions between the two subunits that ensure the stability of the complex. Regardless of changes in the expression of the MPC1 or MPC2 subunits, the final outcome was the decreased activity of MPC and decreased pyruvate uptake, but whether this change is beneficial or harmful depends on types of disease.

Recently, protein lysine acetylation and deacetylation were shown to play an important role in the regulation of cellular metabolism. We found that protein acetylation levels were increased in HG-treated podocytes and dependent on the time frame and concentration of HG stimulation, which has not been reported before. Acetyl CoA is the major donor of the acetyl groups used in acetylation [31]. Therefore, protein acetylation might be related to acetyl CoA metabolism. In addition to the effects of transcriptional switching and allosteric feedback, MPC levels may be controlled by posttranslational modifications such as lysine acetylation, but this acetylation may have short-term temporal consequences [15]. Although MPC2 was acetylated, inactive MPC activity was found in diabetic mouse hearts and the efficiency of pyruvate transport to the mitochondria was significantly reduced [22]. MPC1 was shown to be acetylated in colon cancer cells [32]. Intriguingly, mice fed a high-fat diet exhibited increased acetylated protein in liver mitochondria, but MPC1 acetylation was reduced [33]. In HG-treated podocytes, the acetylation of MPC2 was increased and intracellular pyruvate accumulated, which were also observed in podocytes treated with UK5099. MPC2 peptides containing acetylation sites at K19, K26, K27 and K122 [22], however, these MPC2 acetylation sites in podocytes require further research. Recent research has demonstrated that SIRT3, a mitochondrial lysine deacetylase is implicated in cell metabolism regulation and playes a role in MPC activity [32–34]. The SITR3-MPC pathway might be a regulatory pathway of metabolism.

Pyruvate is an important three-carbon intermediate in energy metabolism and a central substrate in carbohydrate, fat, amino acid catabolic and anabolic pathways. Recent research has suggested that the concentration of pyruvate in the cytosol could determines MPC activity [35]. In this study, we found that pyruvate accumulated in HG-treated podocytes due to MPC2 acetylation, UK5099 treatment and the knockdown of MPC2. The same trend was observed in the kidney cortex of diabetic mice [36]. Recent studies have reported that aberrant pyruvate transport reprograms intracellular metabolism. Decreased glucose metabolism and the insufficient production of ATP via mitochondrial respiration was showed in MPC1 knockdown mice. Fatty acid oxidation was increased and fatty acid synthesis was decreased to maintaining the energy balance in mitochondrial metabolism [37]. Impaired hepatic gluconeogenesis from pyruvate in liver MPC2-deficient mice and the reinforcement of pyruvate-alanine cycling helped to maintain glycemia [23]. The major source of pyruvate is the last step of glycolysis, in which phosphoenolpyruvate is converted to pyruvate by pyruvate kinase (PK). Pyruvate is transferred to mitochondria through MPC and converted into acetyl CoA through the catalysis of pyruvate dehydrogenase (PDH) to drive ATP production by oxidative phosphorylation. PDH activity is also regulated by pyruvate dehydrogenase kinase (PDK). Pyruvate can also be used to generate lactic acid and thus participates in the process of gluconeogenesis. Pyruvate metabolism is rather complex, and any stimulus in the external environment can change key enzyme or protein activities, leading to disordered intracellular metabolism, including pyruvate metabolism. PKM2 expression and activity were found to be elected in glomeruli from mice with diabetes but not those with DKD, but this effect was reversed in HG-treated podocytes [10]. Phosphorylated PDH is increased in the kidneys of diabetic mice, which is consistent with a reduction in mitochondrial biogenesis and the decreased activity of AMPK, a major energy-sensing marker [38]. PDK4 was activated in cisplatin-treated acute kidney injury, leading to mitochondrial dysfunction and cellular apoptosis [39]. Changes in key enzymes and products related to metabolism will be the focus of our future research. The mechanism by which MPC2 mediates metabolism in HG-treated podocytes would be an interesting topic.

Kidneys are mitochondria-rich organs in the body and consume the second highest level of oxygen when at rest. Glucose is the main mitochondrial fuel for energy production through glycolysis and oxidative phosphorylation in glomeruli [40]. Mitochondrial dysfunction has been reported to play a crucial role in HG-treated podocyte injury, in which promotes the development of DKD [8,10,41]. MMP-dependent ROS generation is critical for a comprehensive assessment of mitochondrial function and cell proliferation [42]. In our study, we showed that MMP levels were lower and that cell apoptosis increased in HG-treated podocytes compared to that in untreated podocytes, which confirmed that mitochondria are closely related to podocyte injury. We previously reported that ATP production was decreased and that levels of ROS were increased in HG-treated podocytes [7]. A reduction in MMP and the generation of ROS have also been correlated [43]. Based on the findings of this study, we initially inferred that HG stimulation leads to mitochondrial metabolic disorder and cellular energy deficiency, which increases the release of apoptosis-related factors, such as the members of caspase cascades and the Bcl-2 protein family [44]. A decreased in the MMP and increased ROS production further lead to cellular damage.

Homeostasis mitochondrial network, which is the balance of mitochondrial fission and fusion, is related to cell survival and death. Dynamin-related protein 1 (Drp1), mitofusin1/2 (Mfn1/2) and Optic atrophy 1 (OPA1), which are components of the mitochondrial fission and fusion machinery, have been implicated in mitochondrial morphological changes that are indispensable for cell death [45]. The apoptotic rate of podocytes was shown to be clearly increased under HG conditions and in DKD [46]. Excessive fragmentation of mitochondria is a well-established observation in HG-treated podocytes. In this study, we found fragmented mitochondria in cultured podocytes with MPC2 dysfunction. Knockdown of Drp1 in podocytes resulted in improved mitochondrial fitness associated with enhanced oxygen consumption and ATP production [8]. ROCK1 activation mediated mitochondrial fission by promoting Drp1 recruitment to the mitochondria [47]. Change in mitochondrial morphology under HG conditions contributed to ROS overproduction and cell death [48]. MPC dysfunction might decrease the energy supply in HG-treated podocytes, leading to mitochondrial fission, ROS overproduction and indirect cell death.

Some limitations of this study are the lack of in vivo experiments and an insufficient number of indicators to test mitochondrial function, such as MPC activity, oxygen consumption rate, and ROS production. We will verify this discovery in animal models and human DKD pathological specimens to ensure the consensus between results collected in vivo and in vitro. In the next experiment, mitochondria-related indicators will be improved. For increasing the accuracy of our results, it would be worthwhile to assess acetylation sites and the regulatory mechanisms of MPC2. We will further determine if the overexpression of MPC2 reverses the damage to HG to podocytes. Whether MPC2 mediates metabolic reprogramming in podocytes in DKD will be a further topic for of exploration.

In conclusion, we demonstrate that MPC2 may mediate mitochondrial dysfunction and cell apoptosis in HG-treated podocytes. Enhancing MPC function to increase the tricarboxylic acid (TCA) cycle may reduce injury in HG-treated podocytes. Moreover, screening for molecules related to MPC activity may contribute to new treatments for DKD.

Declaration of competing interest

The authors declare that there is no conflict of interest. Jun Feng, Yiqiong Ma and Guohua Ding conceived and designed the research. Jun Feng and Yiqiong Ma performed the experiments. Zhaowei Chen provided methodology. Jijia Hu and Qian Yang contributed to materials

and analysis techniques. Jun Feng, Yiqiong Ma and Guohua Ding wrote and edited the manuscript. All authors participated in discussing this manuscript.

Acknowledgements

This study was supported by National Natural Science Foundation of China (No.81800615 to Yiqiong Ma, No.81770687 and No.81570617 to Guohua Ding).

Appendix A. Supplementary data

Supplementary data to this article can be found online at https://doi.org/10.1016/j.lfs.2019.116941.

References

[1] E.W. Gregg, Y. Li, J. Wang, N.R. Burrows, M.K. Ali, D. Rolka, D.E. Williams, L. Geiss, Changes in diabetes-related complications in the United States, 1990-2010, N. Engl. J. Med. 370 (2014) 1514–1523.
[2] K.R. Tuttle, G.L. Bakris, R.W. Bilous, J.L. Chiang, I.H. de Boer, J. Goldstein-Fuchs, I.B. Hirsch, K. Kalantar-Zadeh, A.S. Narva, S.D. Navaneethan, J.J. Neumiller, U.D. Patel, R.E. Ratner, A.T. Whaley-Connell, M.E. Molitch, Diabetic kidney disease: a report from an ADA Consensus Conference, Am. J. Kidney Dis. 64 (2014) 510–533.
[3] M. Maqbool, M.E. Cooper, K. Jandeleit-Dahm, Cardiovascular disease and diabetic kidney disease, Semin. Nephrol. 38 (2018) 217–232.
[4] J. Hu, Q. Yang, Z. Chen, W. Liang, J. Feng, G. Ding, Small GTPase Arf6 regulates diabetes-induced cholesterol accumulation in podocytes, J. Cell. Physiol. 234 (2019) 23559–23570.
[5] Y. Abe, T. Sakairi, H. Kajiyama, S. Shrivastav, C. Beeson, J.B. Kopp, Bioenergetic characterization of mouse podocytes, Am. J. Physiol. Cell Physiol. 299 (2010) C464–C476.
[6] C. Tang, Z. Dong, Mitochondria in kidney injury: when the power plant fails, J. Am. Soc. Nephrol. 27 (2016) 1869–1872.
[7] Y. Fan, Q. Yang, Y. Yang, Z. Gao, Y. Ma, L. Zhang, W. Liang, G. Ding, Sirt6 suppresses high glucose-induced mitochondrial dysfunction and apoptosis in podocytes through AMPK activation, Int. J. Biol. Sci. 15 (2019) 701–713.
[8] B.A. Ayanga, S.S. Badal, Y. Wang, D.L. Galvan, B.H. Chang, P.T. Schumacker, F.R. Danesh, Dynamin-related protein 1 deficiency improves mitochondrial fitness and protects against progression of diabetic nephropathy, J. Am. Soc. Nephrol. 27 (2016) 2733–2747.
[9] J. Long, S.S. Badal, Z. Ye, Y. Wang, B.A. Ayanga, D.L. Galvan, N.H. Green, B.H. Chang, P.A. Overbeek, F.R. Danesh, Long noncoding RNA Tug1 regulates mitochondrial bioenergetics in diabetic nephropathy, J. Clin. Investig. 126 (2016) 4205–4218.
[10] W. Qi, H.A. Keenan, Q. Li, A. Ishikado, A. Kannt, T. Sadowski, M.A. Yorek, I.H. Wu, S. Lockhart, L.J. Coppey, A. Pfenninger, C.W. Liew, G. Qiang, A.M. Burkart, S. Hastings, D. Pober, C. Cahill, M.A. Niewczas, W.J. Israelsen, L. Tinsley, I.E. Stillman, P.S. Amenta, E.P. Feener, H.M. Vander, R.C. Stanton, G.L. King, Pyruvate kinase M2 activation may protect against the progression of diabetic glomerular pathology and mitochondrial dysfunction, Nat. Med. 23 (2017) 753–762.
[11] A. Makahleh, G.M. Ben-Hander, B. Saad, Determination of alpha-ketoglutaric and pyruvic acids in urine as potential biomarkers for diabetic II and liver cancer, Bioanalysis 7 (2015) 713–723.
[12] S. Magiera, I. Baranowska, J. Kusa, J. Baranowski, A liquid chromatography and tandem mass spectrometry method for the determination of potential biomarkers of cardiovascular disease, J. Chromatogr. B Anal. Technol. Biomed. Life Sci. 919–920 (2013) 20–29.
[13] M. Aimetti, S. Cacciatore, A. Graziano, L. Tenori, Metabonomic analysis of saliva reveals generalized chronic periodontitis signature, Metabolomics 8 (2012) 465–474.
[14] C. Laustsen, J.A. Ostergaard, M.H. Lauritzen, R. Norregaard, S. Bowen, L.V. Sogaard, A. Flyvbjerg, M. Pedersen, J.H. Ardenkjaer-Larsen, Assessment of early diabetic renal changes with hyperpolarized [1-(13) C]pyruvate, Diabetes Metab. Res. Rev. 29 (2013) 125–129.
[15] T. Bender, J.C. Martinou, The mitochondrial pyruvate carrier in health and disease: to carry or not to carry? Biochim. Biophys. Acta 1863 (2016) 2436–2442.
[16] M.D. Lou, J. Li, Y. Cheng, N. Xiao, G. Ma, P. Li, B. Liu, Q. Liu, L.W. Qi, CREB mediates glucagon action to upregulate hepatic MPC1: inhibitory effect of ginsenoside Rb1 on hepatic gluconeogenesis, Br. J. Pharmacol. 176 (2019) 2962–2976.
[17] Y. Takaoka, M. Konno, J. Koseki, H. Colvin, A. Asai, K. Tamari, T. Satoh, M. Mori, Y. Doki, K. Ogawa, H. Ishii, Mitochondrial pyruvate carrier 1 expression controls cancer epithelial-mesenchymal transition and radioresistance, Cancer Sci. 110 (2019) 1331–1339.
[18] H. Zou, Q. Chen, A. Zhang, S. Wang, H. Wu, Y. Yuan, S. Wang, J. Yu, M. Luo, X. Wen, W. Cui, W. Fu, R. Yu, L. Chen, M. Zhang, H. Lan, X. Zhang, Q. Xie, G. Jin, C. Xu, MPC1 deficiency accelerates lung adenocarcinoma progression through the STAT3 pathway, Cell Death Dis. 10 (2019) 148.
[19] L. Orgaz, G.G. Bueno, Modulating mitochondrial pyruvate carrier: a promising therapeutic target in Parkinson's disease, Mov. Disord. 32 (2017) 719.
[20] J. Kim, L. Yu, W. Chen, Y. Xu, M. Wu, D. Todorova, Q. Tang, B. Feng, L. Jiang, J. He, G. Chen, X. Fu, Y. Xu, Wild-type p53 promotes cancer metabolic switch by inducing PUMA-dependent suppression of oxidative phosphorylation, Cancer Cell 35 (2019) 191–203 e8.
[21] X.P. Tang, Q. Chen, Y. Li, Y. Wang, H.B. Zou, W.J. Fu, Q. Niu, Q.G. Pan, P. Jiang, X.S. Xu, K.Q. Zhang, H. Liu, X.W. Bian, X.F. Wu, Mitochondrial pyruvate carrier 1 functions as a tumor suppressor and predicts the prognosis of human renal cell carcinoma, Lab. Investig. 99 (2019) 191–199.
[22] S.S. Vadvalkar, S. Matsuzaki, C.A. Eyster, J.R. Giorgione, L.B. Bockus, C.S. Kinter, M. Kinter, K.M. Humphries, Decreased mitochondrial pyruvate transport activity in the diabetic heart: role OF mitochondrial pyruvate carrier 2 (MPC2) acetylation, J. Biol. Chem. 292 (2017) 4423–4433.
[23] K.S. McCommis, Z. Chen, X. Fu, W.G. McDonald, J.R. Colca, R.F. Kletzien, S.C. Burgess, B.N. Finck, Loss of mitochondrial pyruvate carrier 2 in the liver leads to defects in gluconeogenesis and compensation via pyruvate-alanine cycling, Cell Metabol. 22 (2015) 682–694.
[24] P.A. Vigueira, K.S. McCommis, G.G. Schweitzer, M.S. Remedi, K.T. Chambers, X. Fu, W.G. McDonald, S.L. Cole, J.R. Colca, R.F. Kletzien, S.C. Burgess, B.N. Finck, Mitochondrial pyruvate carrier 2 hypomorphism in mice leads to defects in glucose-stimulated insulin secretion, Cell Rep. 7 (2014) 2042–2053.
[25] R. Liu, Y. Zhong, X. Li, H. Chen, B. Jim, M.M. Zhou, P.Y. Chuang, J.C. He, Role of transcription factor acetylation in diabetic kidney disease, Diabetes 63 (2014) 2440–2453.
[26] W. Wang, Y. Wang, J. Long, J. Wang, S.B. Haudek, P. Overbeek, B.H. Chang, P.T. Schumacker, F.R. Danesh, Mitochondrial fission triggered by hyperglycemia is mediated by ROCK1 activation in podocytes and endothelial cells, Cell Metabol. 15 (2012) 186–200.
[27] Y. Yuan, A. Zhang, J. Qi, H. Wang, X. Liu, M. Zhao, S. Duan, Z. Huang, C. Zhang, L. Wu, B. Zhang, A. Zhang, C. Xing, p53/Drp1-dependent mitochondrial fission mediates aldosterone-induced podocyte injury and mitochondrial dysfunction, Am. J. Physiol. Renal. Physiol. 314 (2018) F798–F808.
[28] A. Grenell, Y. Wang, M. Yam, A. Swarup, T.L. Dilan, A. Hauer, J.D. Linton, N.J. Philp, E. Gregor, S. Zhu, Q. Shi, J. Murphy, T. Guan, D. Lohner, S. Kolandaivelu, V. Ramamurthy, A. Goldberg, J.B. Hurley, J. Du, Loss of MPC1 reprograms retinal metabolism to impair visual function, Proc. Natl. Acad. Sci. U. S. A. 116 (2019) 3530–3535.
[29] E. Koh, Y.K. Kim, D. Shin, K.S. Kim, MPC1 is essential for PGC-1alpha-induced mitochondrial respiration and biogenesis, Biochem. J. 475 (2018) 1687–1699.
[30] J.C. Schell, K.A. Olson, L. Jiang, A.J. Hawkins, J.G. Van Vranken, J. Xie, R.A. Egnatchik, E.G. Earl, R.J. DeBerardinis, J. Rutter, A role for the mitochondrial pyruvate carrier as a repressor of the Warburg effect and colon cancer cell growth, Mol. Cell 56 (2014) 400–413.
[31] C. Choudhary, B.T. Weinert, Y. Nishida, E. Verdin, M. Mann, The growing landscape of lysine acetylation links metabolism and cell signalling, Nat. Rev. Mol. Cell Biol. 15 (2014) 536–550.
[32] L. Liang, Q. Li, L. Huang, D. Li, X. Li, Sirt3 binds to and deacetylates mitochondrial pyruvate carrier 1 to enhance its activity, Biochem. Biophys. Res. Commun. 468 (2015) 807–812.
[33] A. Li, Q. Liu, Q. Li, B. Liu, Y. Yang, N. Zhang, Berberine reduces pyruvate-driven hepatic glucose production by limiting mitochondrial import of pyruvate through mitochondrial pyruvate carrier 1, EBioMedicine 34 (2018) 243–255.
[34] M.N. Sack, T. Finkel, Mitochondrial metabolism, sirtuins, and aging, Cold Spring Harb. Perspect. Biol. 4 (2012).
[35] V. Compan, S. Pierredon, B. Vanderperre, P. Krznar, I. Marchiq, N. Zamboni, J. Pouyssegur, J.C. Martinou, Monitoring mitochondrial pyruvate carrier activity in real time using a BRET-based biosensor: investigation of the warburg effect, Mol. Cell 59 (2015) 491–501.
[36] K.M. Sas, P. Kayampilly, J. Byun, V. Nair, L.M. Hinder, J. Hur, H. Zhang, C. Lin, N.R. Qi, G. Michailidis, P.H. Groop, R.G. Nelson, M. Darshi, K. Sharma, J.R. Schelling, J.R. Sedor, R. Pop-Busui, J.M. Weinberg, S.A. Soleimanpour, S.F. Abcouwer, T.W. Gardner, C.F. Burant, E.L. Feldman, M. Kretzler, F.R. Brosius, S. Pennathur, Tissue-specific metabolic reprogramming drives nutrient flux in diabetic complications, JCI Insight 1 (2016) e86976.
[37] S. Zou, L. Zhu, K. Huang, H. Luo, W. Xu, X. He, Adipose tissues of MPC1(+/-) mice display altered lipid metabolism-related enzyme expression levels, Peer J. 6 (2018) e5799.
[38] L.L. Dugan, Y.H. You, S.S. Ali, M. Diamond-Stanic, S. Miyamoto, A.E. DeCleves, A. Andreyev, T. Quach, S. Ly, G. Shekhtman, W. Nguyen, A. Chepetan, T.P. Le, L. Wang, M. Xu, K.P. Paik, A. Fogo, B. Viollet, A. Murphy, F. Brosius, R.K. Naviaux, K. Sharma, AMPK dysregulation promotes diabetes-related reduction of superoxide and mitochondrial function, J. Clin. Investig. 123 (2013) 4888–4899.
[39] C.J. Oh, C.M. Ha, Y.K. Choi, S. Park, M.S. Choe, N.H. Jeoung, Y.H. Huh, H.J. Kim, H.S. Kweon, J.M. Lee, S.J. Lee, J.H. Jeon, R.A. Harris, K.G. Park, I.K. Lee, Pyruvate dehydrogenase kinase 4 deficiency attenuates cisplatin-induced acute kidney injury, Kidney Int. 91 (2017) 880–895.
[40] J.M. Forbes, D.R. Thorburn, Mitochondrial dysfunction in diabetic kidney disease, Nat. Rev. Nephrol. 14 (2018) 291–312.
[41] Y. Yuan, S. Huang, W. Wang, Y. Wang, P. Zhang, C. Zhu, G. Ding, B. Liu, T. Yang, A. Zhang, Activation of peroxisome proliferator-activated receptor-gamma coactivator 1alpha ameliorates mitochondrial dysfunction and protects podocytes from aldosterone-induced injury, Kidney Int. 82 (2012) 771–789.
[42] I. Martinez-Reyes, L.P. Diebold, H. Kong, M. Schieber, H. Huang, C.T. Hensley, M.M. Mehta, T. Wang, J.H. Santos, R. Woychik, E. Dufour, J.N. Spelbrink, S.E. Weinberg, Y. Zhao, R.J. DeBerardinis, N.S. Chandel, TCA cycle and

mitochondrial membrane potential are necessary for diverse biological functions, Mol. Cell 61 (2016) 199–209.
[43] S. Cadenas, Mitochondrial uncoupling, ROS generation and cardioprotection, Biochim. Biophys. Acta Bioenerg. 1859 (2018) 940–950.
[44] Q. Yu, M. Zhang, L. Qian, D. Wen, G. Wu, Luteolin attenuates high glucose-induced podocyte injury via suppressing NLRP3 inflammasome pathway, Life Sci. 225 (2019) 1–7.
[45] L.L. Xie, F. Shi, Z. Tan, Y. Li, A.M. Bode, Y. Cao, Mitochondrial network structure homeostasis and cell death, Cancer Sci. 109 (2018) 3686–3694.
[46] X.X. Wang, M.H. Edelstein, U. Gafter, L. Qiu, Y. Luo, E. Dobrinskikh, S. Lucia, L. Adorini, V.D. D'Agati, J. Levi, A. Rosenberg, J.B. Kopp, D.R. Gius, M.A. Saleem, M. Levi, G Protein-coupled bile acid receptor TGR5 activation inhibits kidney disease in obesity and diabetes, J. Am. Soc. Nephrol. 27 (2016) 1362–1378.
[47] W. Wang, Y. Wang, J. Long, J. Wang, S.B. Haudek, P. Overbeek, B.H. Chang, P.T. Schumacker, F.R. Danesh, Mitochondrial fission triggered by hyperglycemia is mediated by ROCK1 activation in podocytes and endothelial cells, Cell Metabol. 15 (2012) 186–200.
[48] T. Yu, J.L. Robotham, Y. Yoon, Increased production of reactive oxygen species in hyperglycemic conditions requires dynamic change of mitochondrial morphology, Proc. Natl. Acad. Sci. U. S. A. 103 (2006) 2653–2658.